

## Band-gap-confinement and image-state-recapture effects in the survival of anions scattered from metal surfaces

Andrew Schmitz,<sup>1</sup> John Shaw,<sup>1</sup> Himadri S. Chakraborty,<sup>1,\*</sup> and Uwe Thumm<sup>2</sup>

<sup>1</sup>*Center for Innovation and Entrepreneurship, Department of Chemistry and Physics, Northwest Missouri State University, Maryville, Missouri 64468, USA*

<sup>2</sup>*Department of Physics and Astronomy, Kansas State University, Manhattan, Kansas 66502, USA*

(Received 3 February 2010; published 6 April 2010)

The resonant charge transfer process in the collision of hydrogen anions with metal surfaces is described within a single-active-electron wave-packet propagation method. The ion-survival probability is found to be strongly enhanced at two different surface-specific perpendicular velocities of the ion. It is shown that, while the low-velocity enhancement is induced from a dynamical confinement of the ion level inside the band gap, the high-velocity enhancement is due to electron recapture from transiently populated image states. Results are presented for Li(110), Cu(111), and Pd(111) surfaces.

DOI: [10.1103/PhysRevA.81.042901](https://doi.org/10.1103/PhysRevA.81.042901)

PACS number(s): 79.20.Rf, 34.70.+e, 73.20.At

### I. INTRODUCTION

The ion surface-interaction processes are of fundamental interests in technological areas, such as (i) analysis, characterization, and manipulation of surfaces [1], (ii) microfabrication based on reactive-ion etching and ion lithography [2], and (iii) semiconductor miniaturization and the production of self-assembled nanodevices [3]. In these methods the charge transfer between an ion and a surface is a key intermediate step. Furthermore, this charge-transfer process primarily determines the final charge state of the scattered, sputtered, or recoiled ions. It is therefore relevant both in the production of ion beams and for the improvement of various analytical techniques; for example, secondary-ion mass spectrometry, low-energy-ion scattering spectroscopy, and metastable atom deexcitation spectroscopy [4].

The rate of charge transfer between a negative ion and a metal surface sensitively depends on the position of the energetically shifted ion-affinity level and the Fermi energy. The transfer of a single electron, the resonant charge transfer (RCT), occurs when the affinity-level shift enables the transfer of an electron to (from) an unoccupied (occupied) resonant state (that is, equal-energy state) of the substrate [5]. The RCT process has been the focus of a number of experimental studies on various mono- and polycrystalline metal surfaces [6–13] and on other exotic surfaces such as, for example, highly oriented pyrolytic graphite [14]. It has been observed [8], following a theoretical prediction [15], that RCT in ion-metal surface interactions can be strongly suppressed by the projected band gap of the metal. This is because the gap obstructs electron penetration normal to the surface, which is the favorable direction of RCT tunneling. Detailed theoretical studies of RCT dynamics and associated ion-neutralization processes in light of the altering crystallographic properties of the surface were carried out by comparing results of Ag(111) with Ag(100) surfaces [16], and Cu(111) with Cu(100) surfaces [17]. In Ref. [16], theoretical results are shown to agree reasonably well with the measurements [9].

The influence of the surface image states on RCT in ion interactions with metal surfaces in the presence of a band gap were discussed in [18].

In the conventional rate-equation approach, the survival probability of the ion scattered from the surface is determined by integrating the static (fixed-ion) widths of the ion level along the flight trajectory [19]. The inverse of the ion speed enters solely as a factor in the exponent of the survival probability. In reality, the ion neutralization rate depends in a much more delicate way on the ion's velocity via the ion-surface effective interaction time. This dependence is a consequence of the nonadiabatic character of the RCT process at finite projectile speeds. Therefore, in a dynamical scenario the ion's level width must depend on the velocity so that the ion's survival becomes different from the static result. This behavior was predicted [20] and subsequently verified experimentally [9]. The interaction-time effect by itself, however, can only produce a rather monotonic evolution in the survival: the shorter the interaction time, the longer the ion survives. But, given the complexity of the metal's band structure and associated RCT dynamics, this effect must be compounded by other important processes. For instance, (i) it is known that for a static ion the affinity level encounters a repulsion from the metal levels due to its coupling with quantum states of the substrate [15,17]. This adiabatic behavior progressively weakens with the increasing speed of the ion, allowing the affinity level to abandon its adiabatic energy curve and explore parts of the surface electronic spectrum that remain nonresonant for adiabatically slow collisions. This means that the ion speed constitutes a key parameter in determining the quality of ion's interactions with metal levels at close distances. Furthermore, (ii) the incoming ion speed provides the transferred electron with excess (kinetic) energy that can force the electron to populate metal levels far from the ion level. If these metal levels are long lived, they can act as transient electron repositories that can subsequently repopulate the neutralized ion. Both these effects can induce characteristic imprints on the ion's survival probability.

In the present study, a profoundly nonmonotonic survival behavior of a hydrogen anion colliding with different atomically flat metal surfaces is predicted. Two resonance-like

\*himadri@nwmissouri.edu

local enhancements are uncovered as a function of the ion speed perpendicular to the surface that emerge from the dynamical competition between decay and recapture events. Beyond this enhancement region, the survival probability continues to decrease with further increase of the perpendicular speed, contrary to the prediction of the simple interaction-time picture.

## II. PROPAGATION METHODOLOGY

The details of the methodology are given in Ref. [17]. Here, we provide a rather succinct account. The time-dependent electronic wave function  $\Phi(\vec{r}, t; D)$  for the ion-surface combined system, with a dynamically changing separation  $D(t)$  between them, is a solution of the time-dependent Schrödinger equation

$$i\hbar \frac{\partial}{\partial t} \Phi(\vec{r}, t; D) = H \Phi(\vec{r}, t; D), \quad (1)$$

with the Hamiltonian

$$H = -\frac{1}{2} \frac{d^2}{dz^2} - \frac{1}{2} \frac{d^2}{dx^2} + V_{\text{ion}} + V_{\text{surf}}. \quad (2)$$

We use atomic units throughout this work, unless indicated otherwise. The  $x$  and  $z$  axes are respectively oriented in directions parallel and perpendicular to the surface in our two-dimensional (2D) numerical approach, which limits the electronic dynamics to the scattering plane. The  $\text{H}^-$  ion is described by a single-electron model potential  $V_{\text{ion}}$ , which includes the interaction of a polarizable hydrogen core with the active electron [21]. The potential  $V_{\text{surf}}$  is the  $z$ -dependent effective potential for the surface and is modeled on the basis of pseudopotential local-density-approximation calculations [17,22]. The surface is rendered translationally invariant along the  $x$  direction, which is a fair approximation for the simple and noble metal surfaces.

The propagation by one time step  $\Delta t$  yields

$$\Phi(\vec{r}, t + \Delta t; D) = \exp[-iH(D)\Delta t] \Phi(\vec{r}, t; D), \quad (3)$$

where the asymptotic initial wave packet  $\Phi(\vec{r}, t = 0; D = \infty)$  is the unperturbed  $\text{H}^-$  wave function  $\phi_{\text{ion}}(\vec{r}; D)$ , which is an eigenfunction of  $-\frac{1}{2} \frac{d^2}{dz^2} - \frac{1}{2} \frac{d^2}{dx^2} + V_{\text{ion}}$ . The ion-survival amplitude, or autocorrelation, is then calculated by the overlap

$$A(t) = \langle \Phi(\vec{r}, t) | \phi_{\text{ion}}(\vec{r}) \rangle. \quad (4)$$

We employ the split-operator Crank-Nicholson propagation method in conjunction with the unitary and unconditionally stable Cayley scheme to evaluate  $\Phi(\vec{r}, t; D)$  in successive time steps [17,23].

We assume specular reflection of the ion from the surface. The incident ion decelerates along the  $z$  direction, close to the surface, due to the net repulsive interaction between the ion core and the surface atoms. For a given initial (asymptotic) kinetic energy  $E_{\text{ion}}$  and angle of incidence (=angle of exit)  $\Theta$  with respect to the surface plane, we simulate a classical trajectory based on ‘‘Biersack-Ziegler’’ interatomic potentials [17,24]. With the increase of the ion’s kinetic energy, the distance of closest approach of the ion to the surface decreases. This influences the ion survival to some extent by somewhat altering the interactions at close distances [17]. In order to keep the analysis simple, we omit the closest-approach dependence

by ensuring a constant distance of closest approach. This is done by appropriately shifting the trajectory along the  $z$ -direction. All the results presented in this article are obtained by fixing the distance of closest approach to be 1.

Long after the ion’s reflection, the final ion-survival probability from our reduced dimensional (2D) propagation is obtained by

$$P_{2\text{D}} = \lim_{t \rightarrow \infty} |A(t)|^2. \quad (5)$$

Assuming a translationally invariant surface with RCT rates that do not depend on the surface coordinates ( $x$  and  $y$ ), we evaluate the ion-survival probability in full (3D) dimensionality as

$$P_{3\text{D}} = |P_{2\text{D}}|^2. \quad (6)$$

This approximation yielded good comparisons with measurements [16].

## III. RESULTS AND DISCUSSIONS

The  $\text{H}^-$  survival probability for the specular scattering of the ion from the Li(110) surface is presented in Fig. 1(a). Ions with kinetic energies of 1, 2, 3, and 6 keV are considered. Results are plotted as a function of the incident or exit angle  $\Theta$  relative to the surface plane. A broad structure appears in each of the 1- and 2-keV curves that peaks respectively at  $\Theta = 40^\circ$  and  $\Theta = 28^\circ$ . For 3 keV, while this structure moves lower in  $\Theta$  to  $22^\circ$ , the onset of another broader structure at higher angles becomes evident. Finally, both these structures clearly emerge in the 6-keV result.

In Fig. 1(b), we show the survival probability as a function of the asymptotic speed (at large ion-surface distance) of the

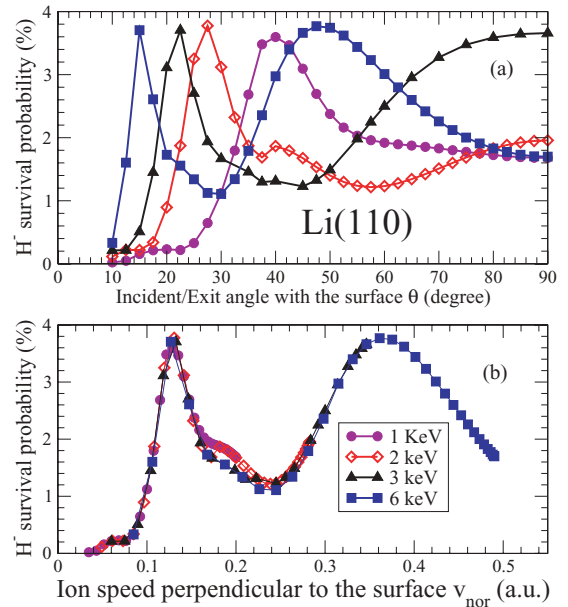


FIG. 1. (Color online) (a) Survival probability of  $\text{H}^-$  specularly scattered from the Li(110) surface as a function of the incident angle with respect to the surface plane. Results are given for four different ion kinetic energies. (b) Same curves as in (a), but as a function of the ion speed normal to the surface.

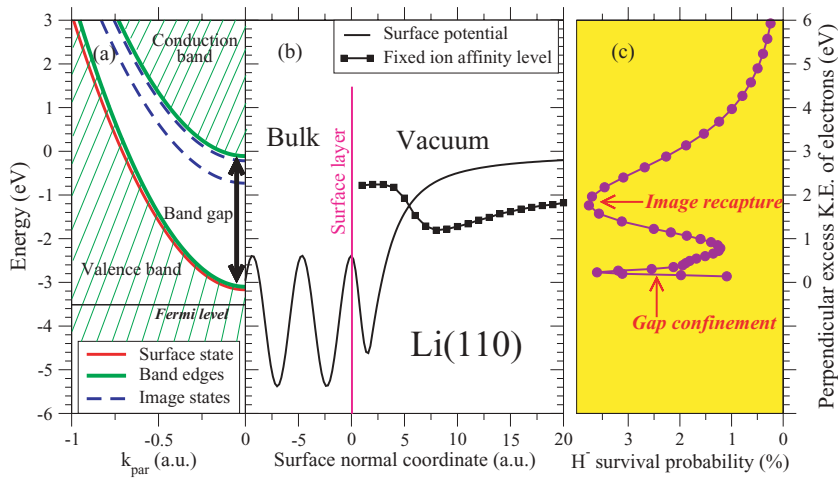


FIG. 2. (Color online) (a) Dispersion relation for Li(110) assuming a translationally invariant surface and an electron-momentum component  $k_{\text{par}}$  in the surface plane. (b) Effective one-dimensional potential for Li(110) as a function of the ion-surface normal coordinate  $z$  and the position of the fixed ion  $\text{H}^-$  affinity level as a function of the ion-surface normal separation  $D$ . The position of the surface along with its bulk and vacuum sides are indicated. (c)  $\text{H}^-$  survival probability as a function of the active electron's excess kinetic energy (in the surface-reference frame),  $0.5(v_{\text{nor}})^2$ , along the direction perpendicular to the surface.

incident ion in the direction perpendicular to the surface:

$$v_{\text{nor}} = \sqrt{\frac{2E_{\text{ion}}}{1836.15}} \sin \Theta. \quad (7)$$

This plot yields a dramatic result. As seen in Fig. 1(b), all the four curves become roughly identical, suggesting a universal behavior of the ion survival as a function of  $v_{\text{nor}}$ : the survival probability is independent of the parallel component of ion velocity. This is due to the fact that our model surface is translationally invariant along the  $x$  direction. This invariance causes the electron transferred from the ion to proceed along the free parallel direction with the same velocity as the ion. Consequently, the parallel relative velocity of the electron with respect to the ion remains zero, causing no kinematic level-shift effect in the electron recapture [25]. Hence, the origin of the two independent structures in the  $\text{H}^-$  survival probability, maximizing at  $v_{\text{nor}} = 0.13$  and  $v_{\text{nor}} = 0.36$ , is the moot question which we try to answer below.

Figure 2(a) presents a schematic dispersion of the electronic band structure of Li(110) with the free continuum parallel to the surface. As seen, this surface has a projected band gap in the surface-normal direction that separates the valence and the conduction band. The gap emerges within the energy range of  $-0.11$  to  $-3.1$  eV with respect to the vacuum level for zero parallel momentum ( $k_{\text{par}} = 0$ ). A Shockley surface state exists that is nearly degenerate with the bottom edge of the band gap. Near the top edge of the band gap, the Rydberg series of image states appears in which the first and the second image states exist inside the gap while the remaining image states are embedded in the conduction band.

In Fig. 2(b), the position of the  $\text{H}^-$  affinity level as a function of fixed ion-surface distances  $D$  is shown. At large  $D$ , the affinity level follows qualitatively the variation of the long-range image part of the surface potential (also shown). However, as the ion moves closer to the surface, its affinity level is energetically repelled by the surface state and valence band states because of its formation of avoided crossings via the interaction through the metal continua. This behavior was previously discussed in wave-packet propagation studies for various metal surfaces [15–17]. The turning point of the affinity level is seen to be at  $D \approx 7$  in Fig. 2(b). Below this value, and until about  $D = 1$ , the affinity level is pushed upward to finally arrive close to the image states near the bottom of

the conduction band. For extremely slow  $v_{\text{nor}}$  (the adiabatic situation), the affinity level is expected to nearly concur with this static behavior and, therefore, will predominantly interact with the image states as well as with the conduction band. Furthermore, since for a very slow ion the interaction time is long, the electron density transferred from the ion to the surface will have enough time to decay through the image state and conduction band continua. This will result in a strongly depleted returning ion and very small survival probability.

As  $v_{\text{nor}}$  increases from its lowest values in Fig. 1(b), the adiabatic approximation begins to fail. As a consequence, the affinity level will progressively plunge deeper into the band gap, mainly following the surface potential before feeling the repulsion. This “delayed” turn-around will ensure that the affinity level cannot have sufficient time to move up to the top of the gap. Thus weaker interactions with metal states will follow, together with an increase in the ion's survival. On the other hand, at larger  $v_{\text{nor}}$ , the affinity level will reach the bottom of the band gap with little to no repulsion such that it directly interacts with the valence band. Neglecting Pauli blocking in our model, the anion then instantly neutralizes by RCT to cause the survival probability to plummet. It is then expected that for a certain intermediate  $v_{\text{nor}}$  the affinity level will effectively dwell at the middle of the gap and hence will experience minimum decay, resulting in a local maximum in the survival probability  $P$ . This indicates the formation of a resonance-like structure in  $P$  in the smaller  $v_{\text{nor}}$  region, as seen in Fig. 1(b), which peaks at  $v_{\text{nor}} = 0.13$ . Since this structure originates from a kind of dynamical confinement of the affinity level inside the band gap, we call it the “gap-confinement effect”.

As  $v_{\text{nor}}$  increases further, another entirely different effect develops that we now discuss. In the perpendicular direction and for a surface-fixed frame of reference, the energy  $E_{\text{nor}}$  of the electron transferred from the ion to the surface at a given distance  $D$  is the sum of the affinity-level energy at  $D$ ,  $\epsilon(D)$ , and the excess kinetic energy the electron acquires from the ion's speed  $v_{\text{nor}}$ :

$$\begin{aligned} E_{\text{nor}} &= \epsilon(D) + \frac{v_{\text{nor}}^2}{2} \\ &= \epsilon(D) + \frac{E_{\text{ion}}}{1836.15} \sin^2 \Theta, \end{aligned} \quad (8)$$

upon using Eq. (7). This positive excess energy [second term on right-hand side of Eq. (8)] represents the kinetic energy of an electron moving with  $v_{\text{nor}}$  in a surface-fixed frame of reference. This frame transformation is the origin of kinematic resonances in capture processes [26] and is of unique importance in the current context. The excess energy can promote the electron to higher states, namely to the image states or the conduction band states, if energetically permissible. Let us be specific. For a value of  $v_{\text{nor}}$  larger than the gap-confinement region, the nonadiabatic condition ensures that the affinity level arrives at the bottom of the band gap at close ion-surface distances. If the ion now releases an electron, then  $\epsilon$  roughly equals  $-3.0$  eV for zero  $k_{\text{par}}$ . At this stage, using Eq. (8), about 2.0 eV of excess energy (corresponding to  $v_{\text{nor}} \approx 0.4$ ) will enable the liberated electron to occupy the first image state [see Fig. 2(a)]. Being localized in the gap, this image state is long-lived and will hold on to the electron long enough to be recaptured by the reflected ion. This effect will enhance the ion's survival. We emphasize that along the outgoing trajectory the affinity level retraces the long-distance part of the surface potential, which energetically facilitates an efficient recapture from the image states.

In Fig. 2(c), we plot the survival probability in front of Li(110) as a function of the excess perpendicular energy of the released electron. We keep a constant parallel speed of 0.2. The gap-confinement effect, discussed above, is seen below 1.0 eV of the excess energy. Above this energy, the survival probability starts growing back again to reach the peak at about 2.0 eV, exactly as anticipated. As the excess energy increases above 2.0 eV, the transferred electron density will be promoted to the conduction band and thereby will progressively favor the decay through the bulk. This will cause  $P$  to diminish again, contrary to the notion of the simple interaction-time model that predicts higher ion survival with faster perpendicular velocity. Obviously, the mechanism of higher recapture of the promoted electron from image states induces a second enhancement that we designate as the “image recapture effect.” Note that the minimum at  $v_{\text{nor}} = 0.26$  between two enhancements signifies the decay of the ion level through the valence band. Ab initio calculations [22,27] estimate the Fermi level of Li(110) to be at about  $-3.4$  eV [Fig. 2(a)]. This being somewhat lower than the bottom ( $-3.1$  eV) of the Li(110) band gap implies that empty levels are available at the top of the valence band. We therefore expect that the inclusion of Pauli blocking in the RCT to the surface would raise, but not eliminate, the minimum of  $P$  at  $v_{\text{nor}} \approx 0.26$ .

In order to further affirm this finding and to examine how the result modifies as the surface band structure alters, we also calculate the  $\text{H}^-$  survival probability for Cu(111) and Pd(111) surfaces. Our results for the Cu(111) surface are presented in Fig. 3(b). The associated surface dispersion, Fig. 3(a), indicates the maximum width of the gap to be about 5 eV, which is roughly double the size of that of Li(110) [Fig. 2(a)]. The broadening of the band gap must strengthen the gap-confinement effect. This is exactly what is seen in Fig. 3(b)—the peak value of the gap-confinement probability in Cu(111) is about twice that for Li(110) [Fig. 2(c)]. The image-recapture effect near Cu(111), however, is weaker than near Li(110). This is because the Cu(111) image states are closer to the conduction band (only the first image state is barely inside

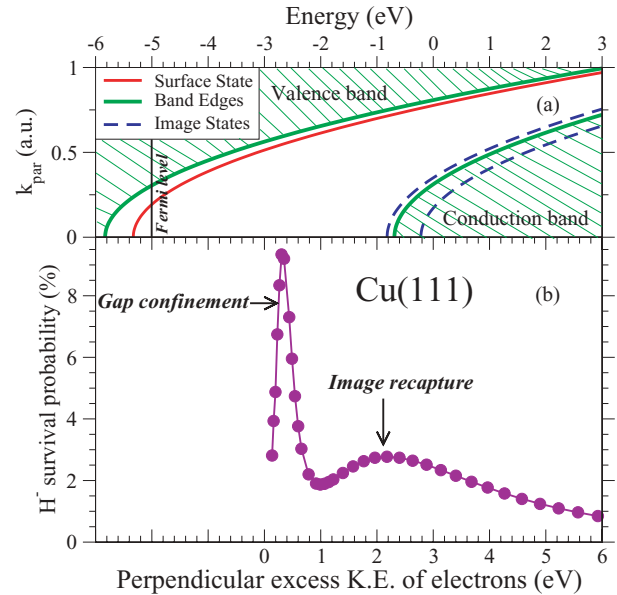


FIG. 3. (Color online) (a) Free-electron dispersion for Cu(111). (b)  $\text{H}^-$  survival probability as a function of the excess kinetic energy perpendicular to the surface (in the surface-reference frame) of the ion-liberated electrons.

the band gap) and consequently are less localized and shorter lived, such that the probability for recapture from image states is smaller. Earlier wave-packet-propagation results for Cu(111) by a different group also suggested two humps in the ion-survival probability (cf. Fig. 3 in [6]). In that work, however, the result from the 2D propagation [Eq. (5)] is plotted, while we use Eq. (6). Therefore, squaring the result of Ref. [6], one finds good agreements of the peak values with the current result [Fig. 3(b)], although there exist differences in details partly due to the inclusion of a velocity-dependent distance of closest approach in [6]. Note further that Pauli blocking is more important near Cu(111), since the Fermi energy ( $\approx -5.0$  eV [22]) of this surface lies above its band-gap bottom [Fig. 3(a)].

For the Pd(111) surface, a significantly different situation arises (Fig. 4). Looking at the Pd(111) band structure in Fig. 4(a), the band gap is seen to extend from 2.0 eV to about  $-4.5$  eV at  $k_{\text{par}} = 0$ . The spectral region of the gap above the vacuum level is largely irrelevant for the formation of the gap-confinement effect, since for the extremely slow adiabatic ion, the electron will primarily decay through the image-state continua during the long ion-surface interaction time. With increasing speed the affinity level will continue to delve energetically deeper in the band gap to build the gap-confinement structure. Therefore, the image-state energies inside the gap will roughly determine the onset of this structure. Hence, considering the size of the Pd(111) gap below the image levels for zero  $k_{\text{par}}$  [Fig. 4(a)], it is not surprising that the peak value of the Pd(111) gap-confinement probability in Fig. 4(b) is intermediate between that of Li(110) and Cu(111). In contrast, the image-recapture enhancement for Pd(111) is remarkably large. This is the consequence of the fact that the whole Rydberg sequence of image states in Pd(111) is located almost at the center of the band gap, in sharp contrast to Li(110) and Cu(111), where the image-state energies are

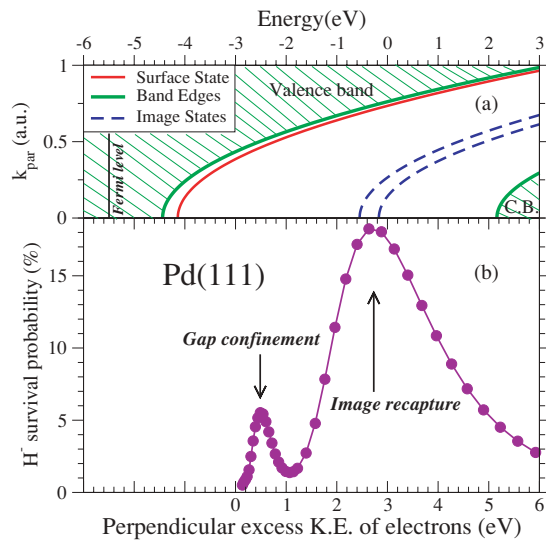


FIG. 4. (Color online) Same as Fig. 3, but for the Pd(111) surface.

close to or degenerate with the conduction band. Evidently, the Pd(111) image states are far more localized and longer lived with a significantly larger electron-retention capability. This ensures strongly enhanced recapture by the outgoing ion, producing a very prominent image-recapture enhancement. For Pd(111), Pauli blocking effects on RCT should be minimal, since the experimentally known Fermi energy for this surface ( $\approx -5.5$  eV [28]) is significantly below the band-gap bottom ( $-4.4$  eV), as shown in Fig. 4(a).

#### IV. CONCLUDING REMARKS

We show that the survival probability of an atomic anion scattered from a plane metal surface is not monotonic as the

simple ion-surface interaction-time model suggests, but structured with band-gap-confinement and image-state-recapture maxima. The former emerges from a spectral confinement of the ion's affinity level inside the metal band gap as the interaction becomes nonadiabatic in character. The later peak is engendered from a boost in the recapture probability as the surface image states are dynamically populated by energetic RCT from the ion. This result must be generic for any metal surface having a band gap closely below or across the vacuum level.

Our result has similarities with the calculations in Ref. [6], as already noted above in the discussion of Fig. 3. However, for higher  $v_{\text{nor}}$ , the survival probability in [6] increases in contra-distinction with our results that show a slow decrease. This decrease in our model is due to the increased access of anion electrons to the metal conduction band, causing quicker decay.

With the change of the distance of closest approach, the gap-confinement structure may significantly alter, since this structure is sensitive to the static-ion energy-position of the affinity level. In contrast, the image recapture peak should persist. Indeed, measurements [6] for high energy  $\text{H}^-$  incidences do suggest a broad hump at larger exit angles. These measurements show no indication of any increase at the high-velocity end of the spectrum, in conformity with the present results. Finally, since Pd(111) exhibits a rather large image-confinement effect, measurements using this surface will be of particular interest.

#### ACKNOWLEDGMENTS

The work is supported by the NSF, an Applied Research Grant from Northwest Missouri State University, and the Division of Chemical Sciences, Office of Basic Energy Sciences, Office of Energy Research, US DOE.

- [1] K. J. Stout and L. Blunt, *Three Dimensional Surface Topography* (Penton Press, London, 2000).
- [2] S. A. Campbell, *The Science and Engineering of Microelectronic Fabrication* (Oxford University Press, New York, 2001).
- [3] *Nanotechnology for Electronic Materials and Devices*, edited by A. Korkin, E. Gusev, J. K. Labanowski, and S. Luryi (Springer, New York, 2007).
- [4] J. W. Rabalais, *Principles and Applications of Ion Scattering Spectrometry: Surface Chemical and Structural Analysis* (Wiley-Interscience, Hoboken, 2003).
- [5] J. P. Gauyacq and A. G. Borisov, *Quantum Dynamics of Complex Molecular Systems*, Chemical Physics, Vol. 83, edited by D. A. Micha and I. Burghardt (Springer, Berlin, 2007), and references therein.
- [6] B. Bahrim, B. Makarenko, and J. W. Rabalais, *Surf. Sci.* **594**, 62 (2005).
- [7] Y. Yang and J. A. Yarmoff, *Phys. Rev. Lett.* **89**, 196102 (2002).
- [8] T. Hecht, H. Winter, A. G. Borisov, J. P. Gauyacq, and A. K. Kazansky, *Phys. Rev. Lett.* **84**, 2517 (2000).
- [9] L. Guillemot and V. A. Esaulov, *Phys. Rev. Lett.* **82**, 4552 (1999).
- [10] E. Sanchez, L. Guillemot, and V. A. Esaulov, *Phys. Rev. Lett.* **83**, 428 (1999).
- [11] S. Ustaze, L. Guillemot, V. A. Esaulov, P. Nordlander, and D. C. Langreth, *Surf. Sci.* **415**, L1027 (1998).
- [12] M. Maazouz, A. G. Borisov, V. A. Esaulov, J. P. Gauyacq, L. Guillemot, S. Lacombe, and D. Teillet-Billy, *Phys. Rev. B* **55**, 13869 (1997).
- [13] F. Wyputta, R. Zimny, and H. Winter, *Nucl. Instrum. Meth. B* **58**, 379 (1991).
- [14] F. Bonetto, M. A. Romerio, E. A. Garcia, R. Vidal, J. Ferrón, and E. C. Goldberg, *Europhys. Lett.* **80**, 53002 (2007).
- [15] A. G. Borisov, A. K. Kazansky, and J. P. Gauyacq, *Phys. Rev. B* **59**, 10935 (1999).
- [16] H. S. Chakraborty, T. Niederhausen, and U. Thumm, *Phys. Rev. A* **69**, 052901 (2004).
- [17] H. S. Chakraborty, T. Niederhausen, and U. Thumm, *Phys. Rev. A* **70**, 052903 (2004).
- [18] H. S. Chakraborty, T. Niederhausen, and U. Thumm, *Nucl. Instrum. Methods B* **241**, 43 (2005).
- [19] J. Los and J. J. C. Geerlings, *Phys. Rep.* **190**, 133 (1990).

- [20] A. G. Borisov, A. K. Kazansky, and J. P. Gauyacq, *Phys. Rev. Lett.* **80**, 1996 (1998).
- [21] V. A. Ermoshin and A. K. Kazansky, *Phys. Lett. A* **218**, 99 (1996).
- [22] E. V. Chulkov, V. M. Silkin, and P. M. Echenique, *Surf. Sci.* **437**, 330 (1999).
- [23] W. H. Press, S. A. Teukolsky, W. T. Vetterling, and B. P. Flannery, *Numerical Recipes: The Art of Scientific Computing* (Cambridge University Press, Cambridge, 2007).
- [24] J. P. Biersack and J. F. Ziegler, *Nucl. Instrum. Methods* **194**, 93 (1982).
- [25] The kinematic level shift is, however, nonvanishing for the occupied metal levels below the Fermi energy [26].
- [26] U. Thumm and J. S. Briggs, *Nucl. Instrum. Methods B* **43**, 471 (1989).
- [27] K. Kokko, P. T. Salo, R. Laihia, and K. Mansikka, *Surf. Sci.* **348**, 168 (1996).
- [28] R. Fischer, S. Schuppler, N. Fischer, T. Fauster, and W. Steinmann, *Phys. Rev. Lett.* **70**, 654 (1993).